Full-band study of current across silicon nanowire transistors

K. Nehari,[a] N. Cavassilas, and F. Michelini
L2MP, UMR CNRS 6137, Bât. IRPHE, 49 Rue Joliot Curie, BP 146, 13384 Marseille Cedex 13, France

M. Bescond
IMEP, UMR CNRS 5130-MINATEC, 3 Parvis Louis Néel, BP 257, 38016 Grenoble Cedex1, France

J. L. Autran and M. Lannoo
L2MP, UMR CNRS 6137, Bât. IRPHE, 49 Rue Joliot Curie, BP 146, 13384 Marseille Cedex 13, France

(Received 5 September 2006; accepted 19 February 2007; published online 28 March 2007)

The authors report an atomistic study of the ballistic current through silicon nanowire metal-oxide-semiconductor transistors. A self-consistent quantum ballistic transport model is used to calculate the current in gate-all-around nanowire transistors, taking into account the full-band structure of the quantum wire with a sp^3 tight-binding approach. The authors demonstrate the occurence of an optimal wire cross section for which the on-state/off-state current ratio is maximum, a result which cannot be obtained in a standard bulk effective mass description. © *2007 American Institute of Physics*. [DOI: 10.1063/1.2716351]

Near the end of the present edition of the International Technology Roadmap for Semiconductor in 2018,[1] the metal-oxide-semiconductor field-effect transistor (MOSFET) will reach the sub-10 nm dimensions. It is widely recognized[2–5] that quantum transport will be a major factor affecting the scaling and the integration of such devices. Particularly, the tunneling contribution to the source-to-drain current will degrade the subthreshold parameters and decrease the on-state/off-state current ratio I_{on}/I_{off}. Multiple-gate structures combined with nanowire conduction channels are expected to be one of the most desirable combination to continue the downscaling of MOSFETs. Indeed the electrostatic control improvement of these architectures has a significant beneficial effect on the current performances.[6]

In such nanowire multiple-gate architectures, electrons are confined in the transverse directions of the wire. As the wire cross section decreases, confinement dramatically modifies the electronic properties in the transport direction and it becomes essential to depict the physics of nanotransistors at the atomic level. Up to now, simulations including the band structure have been essentially based on a semiclassical ballistic model,[7] but usual three-dimensional (3D) quantum mechanical approaches have been still implemented using a bulk effective mass description.[6,8,9]

In this letter, the nanowire transistor current is determined through an atomistic description of the device electronic and transport properties. The system of interest is a gate-all-around (GAA) MOSFET, with a gate length $L_G = 9$ nm, using a silicon nanowire as the conduction channel (Fig. 1) which has already been shown to maximize the device performance.[6] The band structure of this wire is calculated using a sp^3 tight-binding full-band (TBFB) model which leads to transport parameters strongly different from those provided by the bulk effective mass theory.[10] The current across the GAA MOSFET is then computed using these new transport parameters in a 3D self-consistent nonequilibrium Green function (NEGF) quantum transport model.[6]

Let us first give some precisions about the TBFB description. It is based on an orthogonal sp^3 model with up to third-nearest-neighbor interactions and three-center integrals.[11] We use here the parametrization of Ref. 12 which gives an accurate reproduction of the overall bulk band structure and accurate results in the calculation of confined edge states in semiconductor nanostructure of any size. We remind that bulk Si (Ref. 12) is defined by an indirect band gap of 1.143 eV at $k = \pm 0.832.2\ \pi/a_0$ (a_0 is the lattice constant) along the Δ directions with $m_t^* = 0.191 m_0$ and $m_l^* = 0.916 m_0$. The full-band calculations of the wire are performed assuming an infinitely long nanowire with square transverse cross section.

Band structures of square ⟨100⟩-oriented silicon nanowires are calculated for various cross sections (from 1.08×1.08 to 6.3×6.3 nm^2). Transport occurs along the x direction whereas y-z is the confinement plane. Figure 2 shows the E-k_x relations for a nanowire of square cross section 2.72×2.72 nm^2. The quantum confinement splits the six equivalent Δ conduction valleys of the Si bulk band structure into two groups (Fig. 1). The subbands related to the four unprimed valleys Δ_4 ([0±10] and [00±1]) are projected to the Γ point in the one-dimensional Brillouin zone. The subbands related to the primed valleys Δ_2 [±100] are found at higher energies and exhibit a minimum location at $k_x \approx \pm 0.336\ \pi/a_0$. It results that Si nanowires become direct band-gap structures. A nontrivial result is the splitting be-

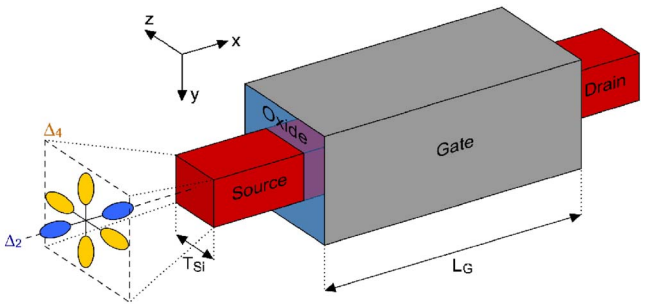

FIG. 1. Schematic view of a Si nanowire MOSFET with a surrounding gate electrode. Electron transport is assumed to be one-dimensional in the x direction. The dimensions of the Si atomic cluster (i.e., the nanowire) under the gate electrode is $[T_{Si}(W=T_{Si})L_G]$ and $L_G = 9$ nm.

[a]Electronic mail: karim.nehari@l2mp.fr

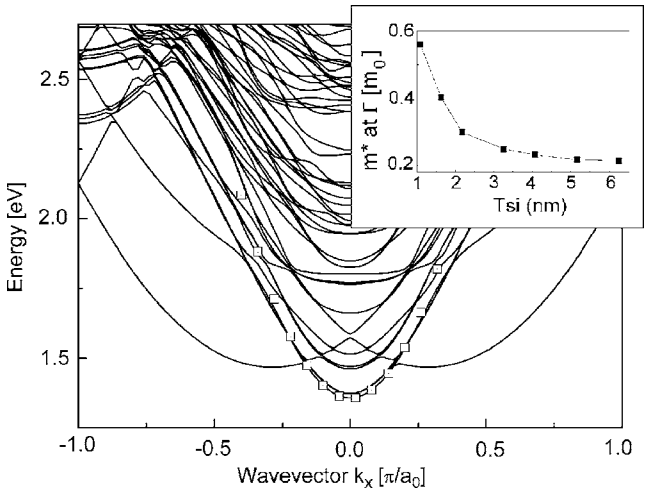

FIG. 2. Energy dispersion relations of the conduction band calculated for 2.72 nm^2 Si wires using the sp^3 tight-binding model. The wire is infinite along the ⟨100⟩ x direction. In square dot (Ref. 5), we show the parabolic approximation. The inset shows the wire width dependence of the transport effective mass m_x^* extracted from the TBFB $E(k_x)$ dispersion relations of the conduction band at the Γ point for the Δ_4 valleys.

tween the subbands associated with the Δ_4 valleys which are expected to be perfectly degenerate. This behavior is discussed in details in Ref. 13.

As shown in Fig. 2, the parabolic approximation of the energy dispersion along the transport direction is still accurate in the energy range of interest for transport in the nanowire (~0.5 eV above the subband edge). The subband positions and the corresponding transport effective masses m_x^* are extracted from full-band calculations as relevant input parameters for the transport model. The inset of Fig. 2 shows m_x^* versus the wire width for the unprimed Δ_4 valleys at the Γ point. The effective mass increases strongly when reducing the wire width. Such a behavior is due to the nonparabolicity of the conduction band in the Si bulk at large k_x.[13]

Using m_x^* and the subband position as input parameters, the current across the GAA MOSFET is calculated considering the nanowire as the conduction channel. The electron density in the channel is obtained from a 3D self-consistent resolution of the Schrodinger-Poisson equations.[10] Electroneutrality is assumed in the contacts which corresponds to Neumann boundary conditions at the source and drain boundaries. To solve the 3D Schrödinger equation, we use the mode-space approach[6,9] which assumes a one-dimensional (1D) transport along the wire axis for each individual subband. It has been shown that this approach gives accurate results as far as the wire cross section is constant. The 1D quantum ballistic transport equation, solved within the NEGF formalism, is then expressed in a simple first neighbor tight-binding model equivalent to the effective mass approach.[6]

We now study the influence of a correct choice of the effective mass on the current calculation. Figures 3 (right) and 4 (right) show the results for the first subband obtained with the bulk masses (m_{bulk}^*) and their tight-binding counterparts for the silicon nanowire (m_{sinw}^*). In both on and off regimes, the first subbands are higher in the m_{sinw}^* case. Such a feature can be explained using the following expression for the 1D electronic density in the source n_S:

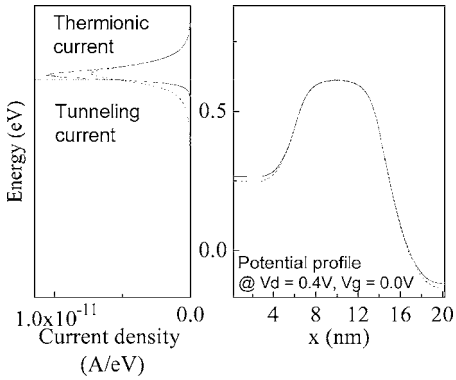

FIG. 3. (Left) Spectral density of current in off-state using sinw m_x^* (solid line) and using bulk m_x^* (dashed line). (Right) Potential profile in off-state along transport direction ⟨100⟩ (source-channel-drain). In this case $W=T_{\text{Si}}=1.2$ nm.

$$n_S = \frac{1}{\pi\hbar\sqrt{2}}\sqrt{m_x^*}\int_{E_{\text{CS}}}^{\infty} E^{-1/2}[(2-T)f_0(E,\mu_S) + Tf_0(E,\mu_D)]dE, \quad (1)$$

where T is the transmission coefficient, μ_S and μ_D are the Fermi levels in the source and drain, respectively, E_{CS} is the conduction band edge in the source, m_x^* the effective mass for the transport, and f_0 the Fermi function. The electronic density n_S is a constant satisfying the electroneutrality law in both reservoirs which are assumed in thermodynamic equilibrium. In Eq. (1), the term under the integral can be taken as a constant both in the on (where $T\approx 1$) and in off regime (where $T\approx 0$). Therefore, to reach self-consistency, E_{CS} must increase with m_x^* to keep n_S in Eq. (1) at the value which ensures electroneutrality in the reservoir (as confirmed by Figs. 3 and 4): using the bulk mass value then leads to underestimated subband positions in source. This argument could be extended to all other regions where the electron density is important as drain access and channel in on state.

In the subthreshold (i.e., off state) regime, the effective mass has not a significant impact on the current calculations. As illustrated in Fig. 3, the maximum of the current density is obtained around the top of the potential barrier. In this regime, the potential in the middle of the channel is not perturbed by a variation of the effective mass. In fact, in this region of the device, in off state, the electron density is weak, so its influence is less important. Moreover, using m_{bulk}^* in-

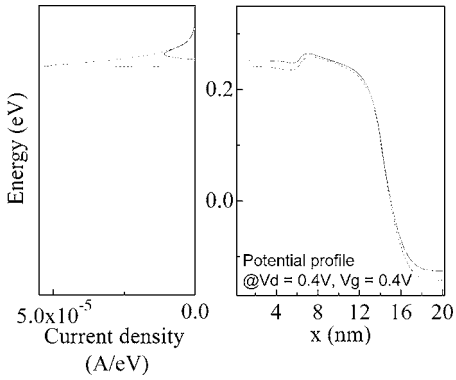

FIG. 4. (Left) Spectral density of current in on-state using sinw m_x^* (solid line) and using bulk m_x^* (dashed line). (right) Potential profile in on-state along transport direction ⟨100⟩ (source-channel-drain). In this case $W=T_{\text{Si}}=1.2$ nm.

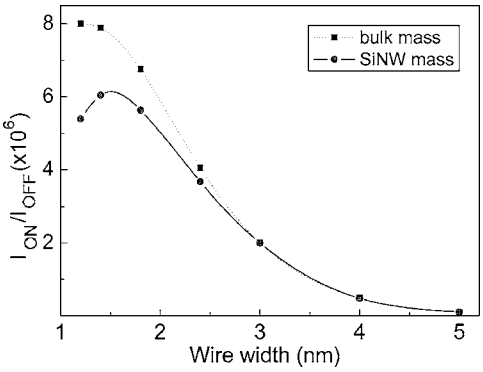

FIG. 5. I_{on}/I_{off} characteristic as a function of the wire width of the nanowire for L_G=9 nm for a gate-all-around architecture with V_D=0.5 V.

duces opposite effects on the current: the tunneling contribution is underestimated while the thermionic contribution is overestimated. Both effects neutralize each other, hence keeping the off-current values constant.

In the upper-threshold regime, including the on state, the potential barrier is significantly higher when the nanowire mass (m^*_{sinw}) is used (Fig. 4). The consequence, as clearly shown on the current spectrum of Fig. 4, is a dramatic reduction of the total current. Using m^*_{bulk} clearly overestimates the on-current value, which prevents from getting reliable results for ultimate dimensions.

We then compute the I_{on}/I_{off} ratio with the two values of the mass (m^*_{sinw} and m^*_{bulk}). The bulk value leads to an increase of the ratio when reducing the cross section followed by a saturation for very small sections (Fig. 5). This can be understood simply since the on-current remains constant (for each 1D channel it is equal to the quantum of conductance times the emission window), while I_{off} decreases since for smaller cross sections one gets better control of the potential which reduces the tunneling current (this effect saturates for very small cross sections). But, for the reasons discussed before, the use of m^*_{bulk} overestimates I_{on} for thin wire. Then using the real effective mass m^*_{sinw}, we get a decrease of I_{on} which explains the peak obtained for I_{on}/I_{off} for ultimate cross sections ($<$1.629 nm).

In conclusion, we demonstrated an optimal section of the silicon nanowire that optimizes the on-state/off-state current ratio. This feature is due to the transport effective mass increase when decreasing cross section ($<$4 nm). Such an optimization is not shown within the silicon bulk effective mass model. Indeed, the strong modification of the band structure in the quantum wire dramatically influences the device transport properties. This shows that reliable predictions for quantum-based devices must rely on full-band atomistic descriptions.

[1] http://public.itrs.net
[2] D. Vasileska and S. S. Ahmed, IEEE Trans. Electron Devices **52**, 227 (2005).
[3] A. Svizhenko, M. P. Anantram, T. R. Govindam, B. Biegel, and R. Venugopal, J. Appl. Phys. **91**, 2343 (2002).
[4] S. Hasan, J. Wang, and M. Lundstrom, Solid-State Electron. **48**, 867 (2004).
[5] S. E. Laux, A. Kumar, and M. V. Fischetti, J. Appl. Phys. **95**, 5545 (2004).
[6] M. Bescond, K. Nehari, J. L. Autran, N. Cavassilas, D. Munteanu, and M. Lannoo, Tech. Dig. - Int. Electron Devices Meet. **2004**, 617.
[7] J. Wang, A. Rahman, A. Ghosh, G. Klimeck, and M. Lundstrom, Appl. Phys. Lett. **86**, 093113 (2005).
[8] M. Bescond, N. Cavassilas, K. Kalna, K. Nehari, L. Raymond, J. L. Autran, M. Lannoo, and A. Asenov, Tech. Dig. - Int. Electron Devices Meet. **2005**, 533.
[9] J. Wang, E. Polizzi, and M. Lundstrom, J. Appl. Phys. **96**, 2192 (2004).
[10] K. Nehari, N. Cavassilas, J. L. Autran, M. Bescond, D. Munteanu, and M. Lannoo, Solid-State Electron. **50**, 716 (2006).
[11] C. Tserbak, H. M. Polatoglou, and G. Theodorou, Phys. Rev. B **47**, 7104 (1993).
[12] Y. M. Niquet, C. Delerue, G. Allan, and M. Lannoo, Phys. Rev. B **62**, 5109 (2000).
[13] T. B. Boykin, G. Klimeck, M. A. Eriksson, M. Friesen, S. N. Coppersmith, P. Von Allmen, F. Oyafuso, and S. Lee, Appl. Phys. Lett. **84**, 115 (2004).